

**Iowa State University**

---

**From the Selected Works of Richard Alan Lesar**

---

September, 1981

# Electronic and vibrational properties of molecules at high pressures. Hydrogen molecule in a rigid spheroidal box

Richard Alan Lesar, *Harvard University*

D. R. Herschbach, *Harvard University*



Available at: [https://works.bepress.com/richard\\_lesar/41/](https://works.bepress.com/richard_lesar/41/)

# Electronic and Vibrational Properties of Molecules at High Pressures. Hydrogen Molecule in a Rigid Spheroidal Box

R. LeSar and D. R. Herschbach\*

Department of Chemistry, Harvard University, Cambridge, Massachusetts 02138 (Received: April 22, 1981;  
In Final Form: June 12, 1981)

A variational calculation employing a five-term James-Coolidge wave function is presented for a hydrogen molecule enclosed within an infinite-walled spheroidal box. Properties examined include the pressure dependence of the equilibrium bond length, the vibrational force constant, the total energy, the ionization potential, the electronic kinetic energy, and the electronic correlation energy. Comparison is made with similar calculations for the  $\text{H}_2^+$  molecular ion and the He and H atoms. A Badger's rule correlation of force constant and bond length is found to hold over a wide pressure range. Comparisons with the available experimental results show that generally the rigid-box model greatly exaggerates the effects of compression.

## I. Introduction

The plight of an atom imprisoned in an infinite-walled box of shrinking volume<sup>1</sup> has long served as a compelling model for study of electronic perturbations induced by high pressure. The prototype example of the hydrogen atom in a spherical box<sup>2</sup> was treated by de Groot and ten Seldam in 1946. Of primary interest were the drastic shifts in the energy levels, the increase in electronic kinetic energy, and the decrease in polarizability on compression. Similar calculations have been done for helium<sup>3</sup> and larger atoms,<sup>4</sup> and other properties have been examined, including hyperfine interactions in the hydrogen atom<sup>5</sup> and the correlation energy of two-electron atoms.<sup>6</sup> The only molecular system previously studied is the hydrogen molecule ion,  $\text{H}_2^+$ , studied first by Cottrell<sup>7</sup> in 1951 and recently more extensively.<sup>8</sup>

This paper gives a variational calculation for a hydrogen molecule in a spheroidal box. In addition to the change with compression of the ground-state electronic energy and bond length, we determined the change in vibrational force constant. The results provide evidence that a quantitative correlation between force constant and bond length holds over a wide range of pressure. This has the same exponential form as an empirical correlation, known as Badger's rule, that holds well for free, gas-phase, diatomic molecules.<sup>9-11</sup> Our calculations were prompted by interest in such a possible correlation, which may prove useful in interpreting vibrational spectra of compressed solids. Large pressure-induced changes in vibrational frequency have been observed recently in solid hydrogen<sup>12</sup> and nitrogen.<sup>13</sup>

We employ the James-Coolidge method<sup>14</sup> with modifications required by the boundary conditions, as outlined in section II and an Appendix. The results for  $\text{H}_2$  are presented in section III and compared with those obtained for  $\text{H}_2^+$  by extending Cottrell's calculations to evaluate the change in vibrational force constant with box size. The Badger's rule correlation and other aspects are discussed in section IV in the context of previous theoretical calculations on solid hydrogen.

## II. Variational Calculations

For molecules in boxes only the vibrational method appears feasible, although for simpler systems some systematic features of exact or perturbative solutions are known.<sup>15</sup> We use the five-term James-Coolidge trial function;<sup>14</sup> for the free  $\text{H}_2$  molecule this function yields more accurate results than a comparable SCF-CI calculation.<sup>16</sup> Unless indicated otherwise, we use standard notation and give all formulas and numerical quantities in atomic units.<sup>17</sup>

The spheroidal box is specified by placing its foci at the two protons (a and b, separated by bond length  $R$ ). The electrons ( $i = 1, 2$ ) are located by prolate spheroidal coordinates ( $\lambda_i, \mu_i, \phi_i$ ). Since surfaces with constant  $\lambda$  are ellipsoids, the boundary of the spheroidal box is specified by  $\lambda = \lambda_0$  and its semimajor axis has length  $1/2 R \lambda_0$ . The potential energy is

$$V = 1/R - 1/r_{a1} - 1/r_{b1} - 1/r_{a2} - 1/r_{b2} + 1/r_{12} \\ = \frac{1}{R} \left[ 1 + \frac{2}{\rho} - 4 \left( \frac{\lambda_1}{\lambda_1^2 - \mu_1^2} + \frac{\lambda_2}{\lambda_2^2 - \mu_2^2} \right) \right] \quad (1)$$

within the box (both  $\lambda_1$  and  $\lambda_2$  in the range 1 to  $\lambda_0$ ), and  $V = \infty$  elsewhere (either  $\lambda_1$  or  $\lambda_2 \geq \lambda_0$ ). The quantity  $\rho = 2r_{12}/R$  is proportional to the interelectronic distance. The variation function has the form

$$\Psi = Ng(\lambda_1, \lambda_2) \Psi_0(\lambda_1, \lambda_2, \mu_1, \mu_2, \rho; R) \quad (2)$$

(1) E. A. Poe, "The Pit and the Pendulum", in *The Gift*, Carey and Hart, Philadelphia, PA, 1842, pp 133-51.

(2) S. R. de Groot and C. A. ten Seldam, *Physica*, **12**, 669 (1946).

(3) C. A. ten Seldam and S. R. de Groot, *Physica*, **18**, 905 (1952).

(4) E. V. Ludeña, *J. Chem. Phys.*, **66**, 468 (1977); **69** (1978).

(5) J. A. Weil, *J. Chem. Phys.*, **71**, 2803 (1979).

(6) E. V. Ludeña and M. Gregori, *J. Chem. Phys.*, **71**, 2235 (1979).

(7) T. L. Cottrell, *Trans. Faraday Soc.*, **47**, 337 (1951).

(8) (a) For an improved variational treatment see K. K. Singh, *Physica*, **30**, 211 (1964); (b) An exact solution for clamped nuclei has now appeared; see E. Ley-Koo and S. A. Cruz, *J. Chem. Phys.*, **74**, 4603 (1981). Comparison with our Table II is not feasible as the authors calculated the energy for  $R = 2a_0$  and did not find the equilibrium bond distance.

(9) R. M. Badger, *J. Chem. Phys.*, **2**, 128 (1934); **3**, 710 (1935); *Phys. Rev.*, **48**, 284 (1935).

(10) D. R. Herschbach and V. W. Laurie, *J. Chem. Phys.*, **35**, 458 (1961).

(11) A. B. Anderson and R. G. Parr, *J. Chem. Phys.*, **53**, 3375 (1970); *Chem. Phys. Lett.*, **10**, 293 (1971).

(12) S. K. Sharma, H. K. Mao, and P. M. Bell, *Phys. Rev. Lett.*, **44**, 886 (1980).

(13) R. LeSar, S. A. Ekberg, L. H. Jones, R. L. Mills, L. A. Schwalbe, and D. Schiferl, *Solid State Commun.*, **32**, 131 (1979).

(14) H. M. James and A. S. Coolidge, *J. Chem. Phys.*, **1**, 825 (1933). See also: W. Kolos and C. C. J. Roothaan, *Rev. Mod. Phys.*, **32**, 219 (1960); W. Kolos and L. Wolniewicz, *J. Chem. Phys.*, **49**, 404 (1965).

(15) I. Gonda and B. F. Gray, *J. Chem. Soc., Faraday Trans. 2*, **71**, 2016 (1975).

(16) F. H. Ree and C. F. Bender, *J. Chem. Phys.*, **71**, 5362 (1979).

(17) Energy: 1 hartree = 2 Ry = 27.21163 eV. Distance: 1 bohr radius = 0.5291772 Å. Force Constant: 1 au = 1.55692 × 10<sup>6</sup> dyn cm<sup>-1</sup>.

Here  $N$  is a normalization factor,  $\Psi_0$  is the five-term James-Coolidge function

$$\Psi_0 = [C_1 + C_2(\mu_1^2 + \mu_2^2) + C_3\mu_1\mu_2 + C_4(\lambda_1 + \lambda_2) + C_5\rho] \exp[-\alpha(\lambda_1 + \lambda_2)] \quad (3)$$

and the cutoff function is

$$g = (\lambda_0 - \lambda_1)(\lambda_0 - \lambda_2) \quad (4)$$

within the box and  $g = 0$  elsewhere. Thus the wave function vanishes at the surface of the box (Dirichlet boundary condition). The boundary condition could be satisfied in other ways, but this choice for  $g(\lambda_1, \lambda_2)$  is convenient; it is analogous to that used by Cottrell for  $H_2^+$ . The  $\Psi_0$  function is symmetric to interchange of electrons ( $^1\Sigma_g^+$  state). The five coefficients  $C_k(R, \lambda_0)$  and exponent  $\alpha(R, \lambda_0)$  are variational parameters.

The matrix elements needed for the variational calculations are evaluated in Appendix A. The integrals must be recalculated for each value of  $\lambda_0$  considered. However, since the integrals do not depend on the internuclear separation  $R$ , except as multiplicative factor, we can readily scan the semimajor axis ( $R\lambda_0/2$ ) and hence the volume of the box for each  $\lambda_0$ . The integrals must also be reevaluated for each choice of the exponent. To reduce computing time, we optimized the exponent for at least three values of  $R$  for each choice of  $R\lambda_0/2$  and used linear interpolation to estimate the exponent for other values of  $R$ . In this way, essentially optimized wave functions and energies were determined as a function of bond length for each  $R\lambda_0$ .

Potential curves were thus obtained, and the location of the potential minima and vibrational force constants were determined by fitting the curves both to a parabolic form and to a three-term Dunham expansion<sup>18</sup>

$$V = a_0\xi^2(1 + a_1\xi + a_2\xi^2) \quad (5)$$

with  $\xi = (R - R_e)/R_e$ . The average kinetic energy was evaluated both directly from the expectation value of the kinetic energy operator and from the virial theorem. For a free diatomic molecule, this provides<sup>19</sup>

$$\bar{T} = -R(\partial E/\partial R) - E \quad (6a)$$

where  $E$  is the total energy. For a spheroidal box, the analogous result<sup>7</sup> is

$$\bar{T} = -R\lambda_0[\partial E/\partial(R\lambda_0)] - E \quad (6b)$$

where the energy derivative with respect to the semimajor axis is evaluated along the locus for which  $(\partial E/\partial R)_{R\lambda_0} = 0$ . The derivatives were obtained by a cubic spline interpolation.

The calculated properties for this box model can be related to pressure by  $P = -\partial E/\partial V$ , where the volume is given by

$$V = (4\pi/3)(\frac{1}{2}R\lambda_0)^3(1 - \lambda_0^{-2}) \quad (7)$$

For large  $\lambda_0$  the spheroid becomes essentially spherical and

$$P \approx (2/\pi)(R\lambda_0)^{-2}|\partial E/\partial(R\lambda_0)| \quad (8)$$

where the energy derivative is again evaluated along the locus of potential minima. The neglect of the second term involving  $\lambda_0^{-2}$  in eq 7 in computing the volume produces an error for the  $H_2$  case of  $\sim 1\%$  for  $R\lambda_0 = 12$  and  $5\%$  for  $R\lambda_0 = 2$ .

Comparison calculations for the  $H_2^+$  molecule ion in a spheroidal box were carried out by using the same varia-

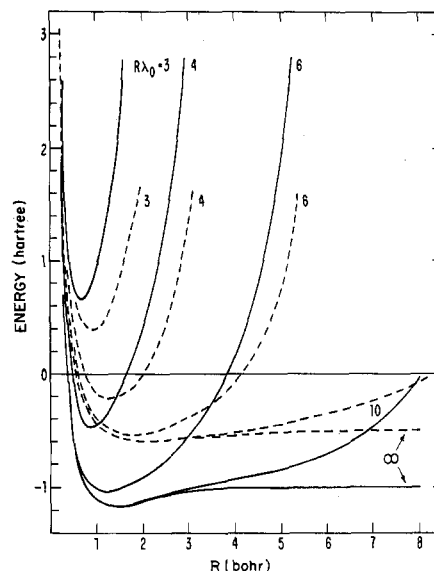


Figure 1. Energy (hartree) of  $H_2$  molecule (solid curves) and  $H_2^+$  molecule ion (dashed curves) in a spheroidal box vs. internuclear distance  $R$  (bohr radius) for a series of box sizes specified by  $R\lambda_0$ , the major axis of the spheroid.

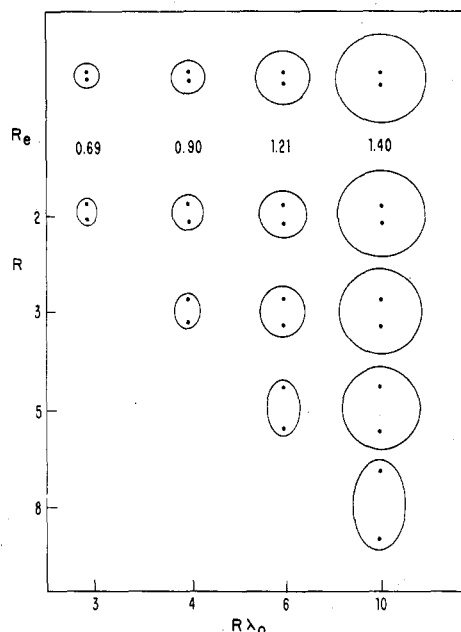


Figure 2. Variation in size and shape of spheroidal box with changes in  $R$  and  $R\lambda_0$  (cf. Figure 1). Dots in each ellipse indicate location of protons. Uppermost row pertains to the equilibrium internuclear distance.

tional function and procedures described by Cottrell.<sup>7</sup> For the energy and equilibrium bond lengths we found the same results at the values of  $R$  and  $\lambda_0$  which he considered. However, we calculated more points along each potential curve in order to determine the vibrational force constant from a fit to a Dunham expansion, eq 5.

### III. Results for $H_2$ and $H_2^+$

Figure 1 shows potential curves (sum of ground-state electronic energy plus nuclear repulsion) as functions of internuclear distance  $R$  for various box sizes designated by the major axis,  $R\lambda_0$ . Along these curves as  $R$  varies the shape of the box changes as well as its size, since the eccentricity  $\lambda_0^{-1}$  of the spheroid must change when  $R\lambda_0$  is fixed. As illustrated in Figure 2, this change in shape indeed corresponds to the mechanism described by Poe<sup>1</sup>

(18) J. L. Dunham, *Phys. Rev.*, **41**, 721 (1932).

(19) J. C. Slater, *J. Chem. Phys.*, **1**, 687 (1933).

TABLE I: Parameters for H<sub>2</sub> in a Spheroidal Box<sup>a</sup>

$R\lambda_0$	$P$	$R_e$	$E_e$	$\bar{T}_e$
$\infty$	0.0 (0)	1.403	-1.1716	1.1716
12	1.6 (0)	1.403	-1.1685	1.1813
10	7.4 (0)	1.395	-1.1638	1.2048
8	5.9 (1)	1.355	-1.1440	1.2999
7	1.7 (2)	1.301	-1.1136	1.4245
6	5.5 (2)	1.208	-1.0441	1.6584
5	1.8 (3)	1.068	-0.8800	2.1111
4	7.7 (3)	0.893	-0.4749	2.9963
3	3.5 (4)	0.686	0.6474	4.9725
2	3.8 (5)	0.455	4.5947	10.6623

<sup>a</sup> All quantities except  $P$  in atomic units.  $R\lambda_0$  is the major axis of the spheroid;  $R\lambda_0 = \infty$  indicates results for free, gas-phase molecule calculated with the same variational function;  $P$  is the pressure (in kbar; to be multiplied by the power of 10 indicated in the parentheses);  $R_e$  is the equilibrium bond length, and  $E_e$  and  $\bar{T}_e$  are the corresponding total electronic energy and average kinetic energy.

TABLE II: Parameters for H<sub>2</sub><sup>+</sup> in a Spheroidal Box<sup>a</sup>

$R\lambda_0$	$P$	$R_e$	$E_e$	$\bar{T}_e$
$\infty$	0.0 (0)	2.024	-0.6022	0.6022
12	2.7 (-1)	2.024	-0.6021	0.6046
10	2.4 (0)	2.012	-0.6010	0.6138
8	2.4 (1)	1.955	-0.5937	0.6594
7	8.0 (1)	1.874	-0.5800	0.7270
6	2.7 (2)	1.731	-0.5455	0.8628
5	9.8 (2)	1.518	-0.1310	1.1224
4	4.1 (3)	1.248	-0.2369	1.6296
3	2.2 (4)	0.936	0.3867	2.7528
2	2.0 (5)	0.601	2.5901	5.9245

<sup>a</sup> Notation and units as in Table I.

("...flatter and flatter grew the lozenge..."). In the well region, however, the box is essentially spherical for all box sizes. As  $R\lambda_0$  decreases, the equilibrium bond length  $R_e$  corresponding to the potential minimum decreases, whereas the energy  $E_e$  at the minimum and the curvature there increase markedly. Comparison of the curves for H<sub>2</sub> and H<sub>2</sub><sup>+</sup> shows two features of interest. Just as with the free, gas-phase molecules,  $R_e$  for H<sub>2</sub> is substantially smaller than for H<sub>2</sub><sup>+</sup> for any box size. However, for sufficiently small boxes, and at large  $R$  for all box sizes,  $E$  for H<sub>2</sub> lies above that for H<sub>2</sub><sup>+</sup>; this indicates that H<sub>2</sub> should undergo ionization in that domain.

Tables I and II list for H<sub>2</sub> and H<sub>2</sub><sup>+</sup> the values of  $E_e$ , the average kinetic energy  $\bar{T}_e$ , and pressure  $P$  corresponding to  $R_e$  for several values of  $R\lambda_0$ . For both H<sub>2</sub> and H<sub>2</sub><sup>+</sup>, the  $\bar{T}_e$  result from eq 6b was verified by a direct evaluation of the expectation value of the Laplacian. A drastic change from the virial relation for a free molecule ( $\bar{T}_e = E_e$ ) occurs as the box shrinks. Figure 3 plots the change in average electronic kinetic energy  $\Delta\bar{T}_e$  as a function of pressure. Also plotted are results for H<sub>2</sub> and He derived from experimental data and a theoretical curve for He atom in a spherical box.<sup>3</sup> For comparison, we include the kinetic energy for two noninteracting electrons in a spheroidal box, calculated as described in Appendix B. At sufficiently high pressures  $\Delta\bar{T}_e$  for the H<sub>2</sub> molecule and He atom appear to converge toward the  $P^{2/5}$  dependence exhibited by two noninteracting electrons.

Figure 4 plots the energy  $E_e$  at the potential minimum as a function of the corresponding box volume,  $V_e$ . For H<sub>2</sub>, the curve remains relatively flat until  $V_e \approx 170a_0^3$  (or  $R\lambda_0 \approx 7a_0$ ); at that point  $E_e$  is  $\sim 0.06$  hartree (or 1.6 eV) higher than the energy of the free molecule. For smaller boxes, the energy climbs rapidly. For H<sub>2</sub><sup>+</sup>, the energy varies more slowly with  $V_e$ ; indeed, this variation is re-

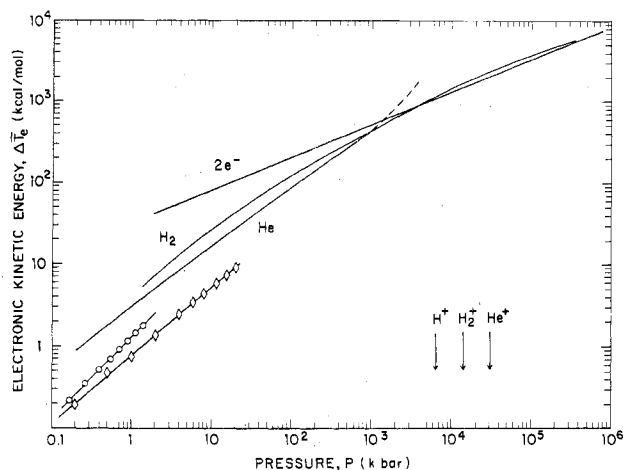


Figure 3. Change in average kinetic energy  $\Delta\bar{T}_e$  (kcal/mol) vs. pressure (kbar) for H<sub>2</sub> molecule and two noninteracting electrons (2e<sup>-</sup>) in a spheroidal box and He atom in a spherical box (ref 3). The result for two noninteracting electrons (given for  $\lambda_0 = 20$ ) shows a linear relation with slope  $2/5$ , as derived in Appendix B. Also shown are the experimental results (O) for H<sub>2</sub> (ref 22) and (◊) for He (calculated here from data of ref 23). The results for He atom in a spherical box show a curious upsurge at  $\sim 1000$  kbar; that may be due to numerical error in the graphical solution employed in ref 3. The arrows indicate the pressure necessary for ionization of H and He atoms (ref 2 and 3) and H<sub>2</sub> molecule, calculated with the box model.

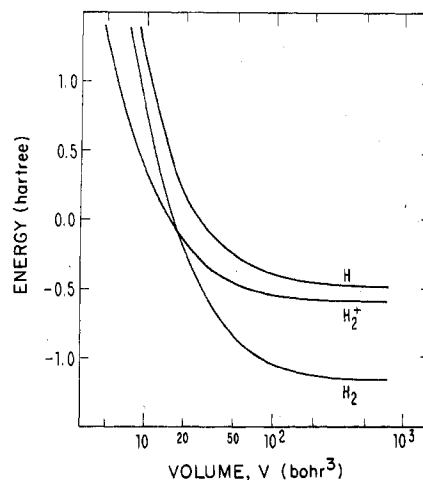


Figure 4. Energy of H<sub>2</sub> and H<sub>2</sub><sup>+</sup> (hartree) at the equilibrium bond length vs. corresponding volume (cubic bohr radius) of spheroidal box compared with the energy of an H atom in a spherical box (from ref 2). The point corresponding to  $r_0 = 1.448$  bohr radii from the H-atom study is not included because that point gave the H-atom curve a large, unphysical bulge.

markably parallel to that for the H atom.<sup>2</sup> The energy of H<sub>2</sub> climbs above that of H<sub>2</sub><sup>+</sup> when  $V_e < 21a_0^3$  (or  $R\lambda_0 < 3.4a_0$ ) and above that of two H atoms when  $V_e \leq 3.8a_0^3$  (or  $R\lambda_0 \leq 2a_0$ ). This indicates that for decreasing box size ionization would occur before dissociation to atoms.

The pressures required to ionize or dissociate the hydrogen molecule may be estimated by comparing the free energy functions,  $G = E + PV$ , for the H<sub>2</sub>, H<sub>2</sub><sup>+</sup>, and H-atom systems. Figure 5 gives these functions. The free energy curves for H<sub>2</sub> and H<sub>2</sub><sup>+</sup> intersect at  $P \approx 14$  Mbar. The corresponding volume change on ionization would be  $\Delta V \approx 6.8a_0^3$  (or  $1.0 \text{ \AA}^3 = 0.60 \text{ cm}^3/\text{mol}$ ). The H<sub>2</sub> and 2H curves do not appear likely to cross unless at pressures well above 100 Mbar.

Figure 6 presents a Badger's rule plot<sup>10</sup> of vibrational force constant vs. equilibrium internuclear distance. Also indicated is a line (shown dashed) obtained from data for

TABLE III: Dunham Parameters for  $H_2$  in a Spheroidal Box<sup>a</sup>

$R\lambda_0$	$a_0$	$a_1$	$a_2$	$B_e$	$\omega_e$	$\omega_e x_e$	$\omega_R$
$\infty$	0.3661	-1.1653	1.7154	60.64	4415	138	4139
12	0.3752	-1.5935	1.4705	60.66	4470	152	4166
10	0.3971	-1.6007	1.2366	61.38	4626	178	4270
8	0.4431	-1.3759	0.9032	65.05	5030	142	4746
7	0.5066	-1.2152	0.6888	70.59	5602	122	5358
6	0.6221	-1.1345	0.6429	81.80	6684	118	6448
5	0.9333	-0.9178	0.3213	104.68	9261	115	9031
4	1.1594	-0.8080	0.3290	148.07	12276	108	12060
3	1.7635	-0.7953	0.3456	253.71	19819	169	19481
2	3.0122	-0.6991	0.3018	576.36	39040	267	38506

<sup>a</sup> The coefficients  $a_0$ ,  $a_1$ , and  $a_2$  are defined in eq 5;  $a_0$  is given in atomic units;  $a_1$  and  $a_2$  are dimensionless;  $B_e$ ,  $\omega_e$ ,  $\omega_e x_e$ , and  $\omega_R$  are in  $\text{cm}^{-1}$  units. The quadratic vibrational force constant is given by  $k_2 = 2a_0/R_e^2 = (1.906 \times 10^{-8})\omega_e^2$ , with  $\omega_e$  in  $\text{cm}^{-1}$ .

TABLE IV: Dunham Parameters for  $H_2^+$  in a Spheroidal Box<sup>a</sup>

$R\lambda_0$	$a_0$	$a_1$	$a_2$	$B_e$	$\omega_e$	$\omega_e x_e$	$\omega_R$
$\infty$	0.2677	-1.5582	1.7152	29.08	2614	57	2500
12	0.2697	-1.5376	1.6621	29.17	2628	56	2516
10	0.2766	-1.5273	1.6451	29.51	2677	56	2665
8	0.3234	-1.3230	0.8320	31.26	2979	63	2853
7	0.3657	-1.1879	1.2146	34.00	3304	28	3248
6	0.4663	-0.9556	0.5941	39.88	4041	33	3975
5	0.6181	-0.9400	1.4842	51.87	5305	-28	5361
4	0.8942	-0.8816	1.0825	76.68	7759	-12	7783
3	1.3973	-0.7542	0.8511	136.27	12929	-28	12985
2	2.4941	-0.6111	0.5661	330.84	26915	-48	27011

<sup>a</sup> Notation and units as in Table III.

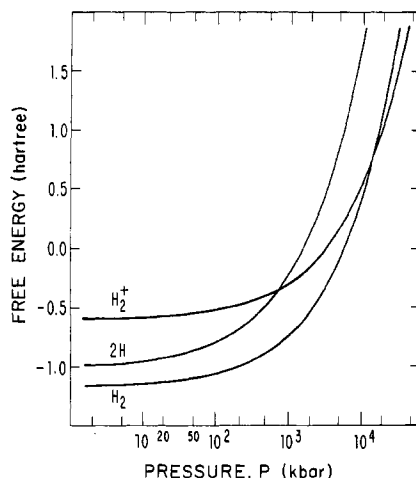


Figure 5. Free energy (hartree) of  $H_2$  and  $H_2^+$  at the equilibrium bond length vs. corresponding pressure (kbar). Also plotted is twice the free energy of an H atom in a spherical box calculated from the results of ref 2 (again omitting the dubious point for  $r_0 = 1.448$  bohr radii).

various electronic states of free, gas-phase  $H_2$  and  $H_2^+$  molecules.<sup>20</sup> Although the force constants for the box systems differ considerably from the gas-phase systems, the plots are again linear except for small boxes ( $R\lambda_0 < 3a_0$ ). In computing the force constants, we found that taking second differences of the energy with respect to the bond length gave good agreement with values obtained by fitting the potential minima to a three-term Dunham expansion. Tables III and IV list the Dunham potential parameters  $a_0$ ,  $a_1$ ,  $a_2$ , the rotational constant  $B_e$ , the vibrational frequency  $\omega_e = (4a_0B_e)^{1/2}$ , the anharmonicity constant  $\omega_e x_e$ , and the corresponding Raman frequency<sup>20</sup>

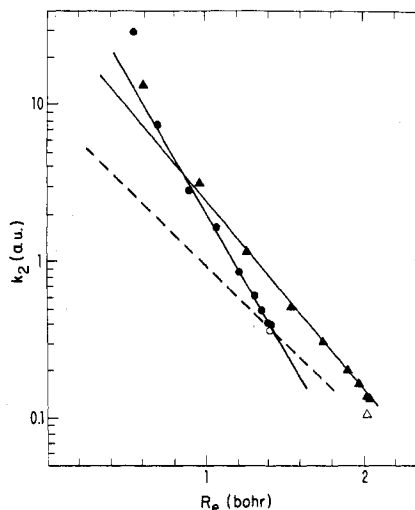


Figure 6. Logarithm of the quadratic vibrational force constant  $k_2$  (atomic units) vs. equilibrium bond length  $R_e$  (bohr radius) for the ground electronic states of (●)  $H_2$  and (▲)  $H_2^+$  in spheroidal boxes. Also shown are the empirical results for (○) the free, gas-phase  $H_2$  molecule and (Δ) the computed result (ref 20) for the free, gas-phase  $H_2^+$  molecular ion. The solid lines were fitted to all but the points at small  $R_e$  for both  $H_2$  and  $H_2^+$ . The dashed line shows the Badger's rule result derived from spectroscopic data for gas-phase  $H_2$  molecules. The lines correspond to  $\log k_2 = mR_e + b$  with  $(m, b) = (-1.77, 2.08)$ ,  $(-1.24, 1.64)$ , and  $(-0.98, 0.96)$  for boxed  $H_2$ ,  $H_2^+$ , and free  $H_2$  or  $H_2^+$ , respectively.

given by  $\omega_R = \omega_e - 2\omega_e x_e$ . This frequency is seen to increase strongly with decrease in box size or increase in pressure.

#### IV. Discussion

In view of the extreme simplicity of the box model, it can offer only a heuristic guide to some aspects of molecular compression. However, the electronic and vibrational properties that can be examined with the box model have in fact been largely ignored in most of the theoretical calculations treating molecular hydrogen at high pressure.<sup>21</sup>

(20) G. Herzberg and L. Huber, "Constants for Diatomic Molecules, Van Nostrand-Reinhold, New York, 1979, pp 240-53; G. Herzberg, "Spectra of Diatomic Molecules", Van Nostrand-Reinhold, New York, 1950.

The intermolecular potential parameters usually used pertain to gas-phase molecules. Few results are available concerning pressure-induced changes of properties such as bond length, vibrational force constant, or electronic correlation energy. Here we compare predictions of the box model for seven properties with quantites and inferences obtained from various theoretical calculations or experiments.

**Electronic Kinetic Energy.** For modest pressures, this quantity permits a rather direct comparison with equation-of-state data. The pressure-induced change  $\Delta\bar{T}$  in the average total kinetic energy can be determined experimentally for a gas at pressure  $P$  and volume  $V$  from

$$\Delta\bar{T} = 3\Delta(PV) - \Delta U \quad (9)$$

where  $U$  is the total energy (for electronic and nuclear motion). At low pressures, where the bond length and vibrational force constant remain essentially unchanged, the contribution to  $\Delta\bar{T}$  from nuclear motion is negligible. Thus Michels and co-workers<sup>22</sup> determined the pressure-induced change  $\Delta\bar{T}_e$  in average electronic kinetic energy for  $H_2$  and other gases by measuring  $\Delta(PV)$  and computing  $\Delta U$  from  $PVT$  data. We have likewise computed  $\Delta\bar{T}_e$  for He from recent data by Mills et al.<sup>23</sup> For  $P = 2$  kbar, the results are  $\Delta\bar{T}_e = 2$  kcal/mol for  $H_2$ , 1.4 kcal/mol for He, and values between 4 and 7 kcal/mol for Ar,  $N_2$ ,  $CO_2$ , and  $C_2H_4$ . For our box model,  $P = 2$  kbar corresponds via eq 8 to  $R\lambda_0 = 11.8$  for  $H_2$ , 10.3 for  $H_2^+$ , and 9.6 ( $2r_0$ , the radius of the sphere) for He, with  $\Delta\bar{T}_e$  of 7.0, 6.4, and 4.6 kcal/mol, respectively. The experimental results for  $H_2$  and He are compared with the box calculations in Figure 3.<sup>24</sup> These results show that the box model exaggerates the effect of compression even for modest pressures.

At high pressures, there is no experimental data from which to evaluate  $\Delta\bar{T}_e$ . The comparison given in Figure 3 indicates that above  $P \approx 100$  kbar, the kinetic energy for both  $H_2$  and He rapidly approaches that for two noninteracting electrons in a box, so that the Coulombic interactions become much less significant than the zero-point energy imposed by the uncertainty principle.

**Molecular Surface Area.** The low-pressure regime allows another application of the virial theorem<sup>25</sup> to derive an effective molecular surface area,  $A$ . In this regime, the potential energy curve for a diatomic molecule can be considered invariant with  $P$ , and eq 6a enables the change in kinetic energy to be related to a change in bond length  $R$  and electronic energy  $\Delta E$ . The effective area  $A$  is obtained by dividing the force required to change the bond length,  $-\partial E/\partial R$ , by the pressure; thus

$$A \approx (\Delta\bar{T} + \Delta E)/RP \quad (10)$$

(21) For a recent review, see: (a) M. Ross and C. Shishkevitch, "Molecular and Metallic Hydrogen", Rand Corp., Santa Monica, CA, 1977; (b) I. F. Silvera, *Rev. Mod. Phys.*, **52**, 393 (1980).

(22) Hydrogen: A. Michels and M. Goudekot, *Physica*, **8**, 387 (1942). Nitrogen: R. J. Lunbeck, A. Michels, and G. J. Wolters, *Appl. Sci. Res., Sect. A*, **3**, 197 (1952). Argon: A. Michels, R. J. Lunbeck, and G. J. Wolters, *ibid.*, **2**, 345 (1951). Carbon Dioxide: A. Michels and S. R. de Groot *ibid.*, **1**, 94, 103 (1949). Ethylene: A. Michels, S. R. de Groot, and M. Geldermans, *ibid.*, **1**, 55 (1946); *Physica*, **12**, 105 (1946).

(23) R. L. Mills, D. H. Liebenberg, and J. C. Bronson, *Phys. Rev. B*, **21**, 5137 (1980). The equation of state given here is good above 1 kbar, so the internal energy was calculated with respect to the value there. The value at 1 kbar was found by extrapolation of the data of S. W. Akin, *Trans. ASME*, **72**, 751 (1950).

(24) A similar comparison for He over a much smaller range of pressures was given by ten Seldam and de Groot (ref 3). They found for  $P = 0.5$  kbar an experimental  $\Delta\bar{T}_e = 0.5$  kcal/mol whereas the box calculation gave 2 kcal/mol.

(25) T. L. Cottrell, *J. Chem. Phys.*, **18**, 1117 (1950); J. O. Hirschfelder, C. F. Curtiss, and R. B. Bird, "Molecular Theory of Gases and Liquids", Wiley, New York, 1954, pp 264-8.

TABLE V: Estimates of Correlation Energy for  $H_2$  and He<sup>a</sup>

$R\lambda_0$	$\Delta E_\rho(H_2)$	$\Delta E_c(He)$	$\Delta E_\rho/\Delta E_c$
$\infty$	-0.0200	-0.0409	0.49
12	-0.0209	-0.0409	0.51
10	-0.0214	-0.0408	0.52
8	-0.0224	-0.0407	0.55
6	-0.0246	-0.0402	0.61
4	-0.0279	-0.0401	0.70
2	-0.0281	-0.0435	0.65

<sup>a</sup> Hartree atomic units.  $\Delta E_\rho(H_2) = E_5 - E_4$ , where  $E_5$  is the energy for  $H_2$  at  $R_0$  (given in Table I) computed with the five-term variational function of eq 13 and  $E_4$  is the energy obtained by omitting the term involving  $C_{5\rho}$ .  $\Delta E_c(He)$  is the correlation energy for He in a spherical box (ref 6) with radius  $r_0 = 1/2 R\lambda_0$ .

For  $H_2$  this yields  $A \approx 90 \text{ \AA}^2$  for  $P = 2$  kbar, with the use of the experimental  $\Delta\bar{T} = 2$  kcal/mol and a theoretical value  $\Delta E = 0.005$  kcal/mol derived from the Kolos-Wolniewicz<sup>14</sup> potential. From the box model

$$A = 4\pi(1/2 R\lambda_0)^2 [1 - \lambda_0^{-2} + \lambda_0(1 - \lambda_0^{-2})^{1/2} \sin^{-1}(1/\lambda_0)] \quad (11)$$

For  $P = 2$  kbar, we find  $A \approx 120$  and  $90 \text{ \AA}^2$  for  $H_2$  and  $H_2^+$ , respectively. The corresponding  $\Delta E = 2.26$  and  $0.65$  kcal/mol. These numbers show that the box model not only exaggerates  $\Delta\bar{T}$  and  $\Delta E$  but also predicts the ratio  $\Delta\bar{T}/\Delta E$  to be much smaller (3.72 for  $H_2$ ) than the ratio found from experimental data (400 for  $H_2$ ). It is remarkable that at low pressures the box model manages to overdo so much the effects of compression, despite also overestimating substantially the molecular surface area.

**Electron Correlation Energy.** Table V provides a comparison with calculations done for two-electron atoms in spherical boxes.<sup>6</sup> The correlation energy was found to increase only slightly as the box shrinks. Our five-term variational function yields an energy for the unboxed  $H_2$  molecule that is within 0.0029 hartree of the exact result.<sup>14</sup> However, since Hartree-Fock energies are not available for the boxed molecule, we cannot evaluate the correlation energy in the usual way,  $\Delta E_c = \Delta E_{\text{exact}} - \Delta E_{\text{HF}}$ . Instead, we tabulate the difference between calculations done with and without the term proportional to the interelectronic separation  $C_{5\rho}$  in eq 3; this difference  $\Delta E_\rho$  is expected to be at least roughly proportional to  $\Delta E_c$ . For unboxed  $H_2$ , the correlation energy is 0.04083 hartree<sup>16</sup> and thus  $\Delta E_\rho/\Delta E_c = 0.489$  there. The gradual increase in  $\Delta E_\rho$  as the box shrinks is remarkably parallel to that in the correlation energy for helium; indeed,  $\Delta E_\rho(H_2)/\Delta E_c(He) = 0.6$  within 0.1 over the full range of box sizes. In view of the large increase in the electronic energy (Table I), these results indicate that electron correlation or repulsion energy becomes relatively much less important at high compressions, despite the shrinking volume accessible to the electrons.

**Transition to Metallic Phase.** Since the prediction of a high-pressure transition to a metallic hydrogen phase by Wigner and Huntington in 1935,<sup>26</sup> this phenomenon has been explored in many calculations and at least three experiments.<sup>12,27</sup> Estimates of the transition pressure range

(26) E. Wigner and H. B. Huntington, *J. Chem. Phys.*, **3**, 764 (1935). The original suggestion of a high-pressure nonmetal-metal transition was made earlier by K. F. Herzfeld, *Phys. Rev.*, **29**, 701 (1927).

(27) F. V. Grigor'ev, S. B. Kormer, O. L. Mikhailova, A. P. Tolochko, and V. D. Ustin, *Pis'ma Zh. Eksp. Teor. Fiz.*, **16**, 286 (1972) (*JETP Lett. (Engl. Transl.)*, **16**, 201 (1972)); P. S. Hawke, T. J. Burgess, D. E. Duerre, J. G. Hebel, R. N. Keela, H. Klapper, and W. C. Wallace, *Phys. Rev. Lett.*, **41**, 994 (1978).

from 0.2 to 4 Mbar; tentative theoretical consensus and experimental evidence now indicate  $\sim 2$  Mbar.<sup>28</sup> Most theoretical treatments consider the transition as (a) first order with a volume change  $\Delta V$  on the order of  $0.5 \text{ cm}^3/\text{mol}$  and (b) occurring directly from the molecular phase to a conducting atomic phase. However, some treatments suggest that the transition is (a') more gradual and/or (b') the molecular phase itself becomes conducting.<sup>29</sup> As shown in Figure 5, the box model predicts a first-order transition at  $P \approx 14$  Mbar with  $\Delta V = 0.67 \text{ cm}^3/\text{mol}$  to form a conducting molecular phase based on the  $\text{H}_2^+$  ion. The work of Singh<sup>8</sup> suggests that a better variational function for  $\text{H}_2^+$  may lower the transition pressure, though comparison of the free energy vs. pressure relation in the two calculations shows little difference, the result with Cottrell's function having a slightly lower free energy at the highest pressure studied by Singh (12 kbar). In view of its propensity to exaggerate effects of compression, the box model yields surprisingly plausible results for the phase transition.

**Pressure-Induced Changes in  $R_e$  and  $\omega_e$ .** At present, no other calculations seem to be available for the pressure dependence of the equilibrium bond length and vibrational frequency. The box model predicts (Tables I–IV) large pressure-induced changes in all of the parameters required to describe the rotational and vibrational motion. For  $\text{H}_2$  and  $\text{H}_2^+$ , a 5-fold decrease in the box major axis produces about a  $\sim 10$ -fold increase<sup>30</sup> in both the rotational constant  $B_e$  and the vibrational frequency  $\omega_e$ . There is no experimental information about  $R_e$  or  $B_e$ . Raman spectra obtained by Sharma, Mao, and Bell<sup>12</sup> show that the vibrational bond stretching frequency of  $\text{H}_2$  increased by  $\sim 110 \text{ cm}^{-1}$  as the pressure increased up to 300 kbar (at room temperature) and then decreased by  $\sim 25 \text{ cm}^{-1}$  with further pressure increase up to 630 kbar (the maximum pressure obtained). The initial increase is attributed to compressive shortening and stiffening of the molecular bond,<sup>31</sup> and the decrease at high pressure perhaps to the onset of molecular dissociation. A Hartree–Fock study of solid  $\text{H}_2$  by Ramaker, Kumar, and Harris<sup>29</sup> indeed found a gradual weakening and lengthening of the bond at very high pressures and a transition to the metallic phase at  $\sim 2.1$  Mbar. The box model predicts that the  $\text{H}_2$  Raman frequency  $\omega_R$  (Table III) increases by  $\sim 2100 \text{ cm}^{-1}$  as the pressure climbs to 300 kbar and continues to increase until the neighborhood of the phase transition at 14 Mbar, where the  $\text{H}_2 \rightarrow \text{H}_2^+$  transformation produces a large increase in  $R_e$  (by 65%) and a decrease in  $\omega_R$  (by 33%). Thus, again the box model caricatures the trends.

**Badger's Rule Correlation.** As seen in Figure 6, the box model predicts an accurately semilogarithmic correlation between  $R_e$ , the equilibrium bond length, and  $k_2$ , the quadratic vibrational force constant. This holds over the full range of box size or pressure, until the phase transition sets in (near  $R_{\lambda_0} \approx 3a_0$ ). The slope of the correlation,  $\partial \log k_2 / \partial R_e$ , is similar for  $\text{H}_2$  and  $\text{H}_2^+$  but is about twice as steep as that found empirically for the free, gas-phase

molecules. This suggests that Badger's rule can be used to infer changes in bond length from changes in vibrational frequency for compressed molecules, but the appropriate slope may be somewhat larger than for the gas-phase case. For instance, in this way we estimate that an increase in  $\omega_R$  by  $\sim 100 \text{ cm}^{-1}$  corresponds to a decrease in  $R_e$  by  $\sim 0.01a_0$  (0.8%) according to the box-model correlation or  $\sim 0.02a_0$  (1.4%) according to the gas-phase Badger's rule.

The bond stretching frequency in solid nitrogen also increases with pressure,<sup>13</sup> by  $\sim 55 \text{ cm}^{-1}$  up to 370 kbar. From Badger's rule with gas-phase parameters,<sup>10</sup> this frequency corresponds to a decrease in bond length by  $\sim 0.02a_0$  (1%), comparable to that for  $\text{H}_2$ . This contrasts with a recent ab initio calculation,<sup>32</sup> which found that placing two  $\text{N}_2$  molecules  $5a_0$  apart increased the vibrational frequency by 6000  $\text{cm}^{-1}$  but decreased the equilibrium bond length by only  $0.0265a_0$  (1.2%). Since these numbers imply a Badger's rule slope on the order of  $10^4$  times larger than the empirical value,<sup>10</sup> the ab initio prediction appears outlandish.

**Assessment.** Should the verdict on the box model be "nevermore"? Despite its failings, we think not. The excellent experimental studies now available for electronic<sup>33</sup> and vibrational<sup>12,13</sup> properties of compressed molecules require a practical theoretical approach, and other current methods also have severe limitations. The box model might be improved by replacing the "hard-cell" model considered here by a "padded-cell" model, in which the potential at the boundary surface of the box has a finite value. This boundary potential as well as the size of the box could be determined from experimental PVT data and the model thus calibrated used to predict other properties.<sup>34</sup> Another improvement would be to make the box size and shape independent of the location of the atomic nuclei. Here, in order to retain simple boundary conditions for computing the variational integrals, we followed Cottrell<sup>7</sup> and fixed the protons at the foci of the spheroid. A more general formulation would add flexibility and permit study of the pressure-induced "freezing-out" of molecular rotations.<sup>35</sup>

**Acknowledgment.** We thank Dr. Susanne Raynor for helping us compress some of the matrix computations. We are grateful for support of this work by the Department of Energy under Contract DE-AC02-79ER10470.

## Appendix A

We describe here only aspects of the calculation affected by the spheroidal box; for other aspects and notation see the work of James and Coolidge.<sup>14</sup>

All of the necessary integrals can be written in terms of the quantities

$$Z^r(m, n, j, k, p) = (4\pi^2)^{-1} \iiint \iiint \iiint I \, d\lambda_1 \, d\lambda_2 \, d\mu_1 \, d\mu_2 \, d\phi_1 \, d\phi_2 \quad (\text{A1})$$

(28) F. H. Ree and N. W. Winter, *J. Chem. Phys.*, **73**, 322 (1980).

(32) F. H. Ree and N. W. Winter, *J. Chem. Phys.*, **73**, 322 (1980).  
(33) G. Webster and H. G. Drickamer, *J. Chem. Phys.*, **72**, 3740 (1980);  
G. Chrysomallis and H. G. Drickamer, *Chem. Phys. Lett.*, **67**, 381 (1979);  
*J. Chem. Phys.*, **71**, 4817 (1979).

(34) For instance, one possibility suggested by Figure 3 is to use the  $\Delta T_e$  derived from experiment to recalibrate the pressure scale. For the rigid-box model, this would reduce the predicted change  $\Delta\omega_R$  in  $\text{H}_2$  vibration frequency at 300 kbar from  $2100 \text{ cm}^{-1}$  to only  $\sim 400 \text{ cm}^{-1}$ . For a finite-walled box,  $\Delta\omega_R$  might be substantially smaller, but a consistent procedure for assigning the box size and potential step remains to be devised.

(35) J. C. Raich and R. D. Ethers, *J. Low Temp. Phys.*, **6**, 229 (1972);  
W. England, J. C. Raich, and R. D. Ethers, *ibid.*, **22**, 213 (1976).

(36) C. Zener and V. Guillemin, *Phys. Rev.*, **34**, 999 (1929); N. Rosen, *ibid.*, **38**, 2099 (1931).

(28) For example: M. Ross, *J. Chem. Phys.*, **60**, 3634 (1974); R. D. Ethers, R. Danilowicz, and W. England, *Phys. Rev. A*, **12**, 2199 (1975). See ref 21a for other references.

(29) D. E. Ramaker, L. Kumar, and F. E. Harris, *Phys. Rev. Lett.*, **34**, 812 (1975); C. Friedli and N. W. Ashcroft, *Phys. Rev. B*, **16**, 662 (1977).

(30) The large increase in vibrational frequency (the quantum becomes  $\sim 5 \text{ eV}$  at  $R_{\lambda_0} = 2$  bohr radii) raises the question whether the Born–Oppenheimer approximation remains valid as the box shrinks. This depends on the ratio  $T_n/T_e$  of the nuclear kinetic energy to the electronic kinetic energy. On computing  $T_n$  taking only the  $a_0$  term of the Dunham potential and dividing by  $T_e$  from Table I, we find that the ratio remains small ( $\sim 4 \times 10^{-3}$ ) and roughly constant as the box shrinks.

(31) E. Whalley, *Proc. Int. Conf. High Pressure*, 4th, 1974, 37 (1975).

where the integrand is

$$I = \lambda_1^m \lambda_2^n \mu_1^j \mu_2^k \rho^p \exp[-\delta(\lambda_1 + \lambda_2)] M^p \cos^p(\phi_1 - \phi_2)$$

with  $\delta = 2\alpha$  and

$$M^2 = (\lambda_1^2 - 1)(\lambda_2^2 - 1)(1 - \mu_1^2)(1 - \mu_2^2)$$

Our choice of cutoff function,  $g(\lambda_1, \lambda_2) = (\lambda_0 - \lambda_1)(\lambda_0 - \lambda_2)$ , introduces terms only of the standard type and changes the upper limits for the  $\lambda_1$  and  $\lambda_2$  integration to  $\lambda_0$  instead of infinity.

There are two kinds of  $Z^p$  integrals that we need to consider.

(a) The  $p = 0$  case:

$$Z^0(m, n, j, k, 0) = 4A_m(\delta) A_n(\delta) / [(k+1)(j+1)]$$

for  $j$  and  $k$  even; this is zero for  $j$  or  $k$  odd. Also

$$Z^1(m, n, j, k, 0) = 0$$

for any  $j$  and  $k$ . Here

$$\begin{aligned} A_m(\alpha) &= \int_1^{\lambda_0} e^{-\alpha\lambda} \lambda^m d\lambda \\ &= A_m(1; \alpha) - A_m(\lambda_0; \alpha) \end{aligned} \quad (\text{A2})$$

with

$$\begin{aligned} A_m(x; \alpha) &= \int_x^{\infty} e^{-\alpha\lambda} \lambda^m d\lambda \\ &= (m!/\alpha^{m+1}) \exp(-\alpha x) \sum_{\nu=0}^m (\alpha^\nu/\nu!) x^\nu \end{aligned} \quad (\text{A3})$$

For a free, gas-phase molecule  $\lambda_0 \rightarrow \infty$  and  $A_m(\lambda_0; \delta) \rightarrow 0$ .

(b) The  $p = -1$  case:

$$Z^0(m, n, j, k, -1) = \sum_{\tau=0}^{\infty} (2\tau+1) R_\tau(j) R_\tau(k) H_\tau(m, n, \delta)$$

$$Z^1(m, n, j, k, -1) =$$

$$-\sum_{\tau=1}^{\infty} [(2\tau+1)\tau^{-2}(\tau+1)^{-2}] R_\tau^1(j) R_\tau^1(k) H_\tau^1(m, n, \delta)$$

where the  $R_\tau$  quantities are given by James and Coolidge; only a few are nonzero so the summations reduce to a few terms. For the  $H_\tau$  quantities, James and Coolidge provide a recursion relation that permits them all to be expressed in terms of two simpler integrals

$$\begin{aligned} H_0(m, n, \delta) &= \\ A_m(\delta) F_n(\delta) + A_n(\delta) F_m(\delta) - T(m, n, \delta) - T(n, m, \delta) \end{aligned} \quad (\text{A4})$$

$$S(m, n, \delta) =$$

$$(m!/\delta^{m+1}) \sum_{\nu=0}^m (\delta^\nu/\nu!) A_{n+\nu}(2\delta) - A_m(\lambda_0; \delta) A_n(\delta) \quad (\text{A5})$$

Here

$$F_m(\delta) = \int_1^{\lambda_0} Q_0(\lambda) e^{-\delta\lambda} \lambda^m d\lambda \quad (\text{A6})$$

with

$$Q_0(\lambda) = \frac{1}{2} \ln [(\lambda+1)/(\lambda-1)]$$

$$T(m, n, \delta) =$$

$$(m!/\delta^{m+1}) \sum_{\nu=0}^m (\delta^\nu/\nu!) F_{n+\nu}(2\delta) - A_m(\lambda_0; \delta) F_n(\delta) \quad (\text{A7})$$

The  $F$  integrals for  $\lambda_0 = \infty$  are available,<sup>36</sup> for  $\lambda_0 < \infty$ , we have

$$\begin{aligned} F_m(\delta) &= \frac{1}{2} [\ln(2\delta) + \gamma - Ei[-\delta(\lambda_0 - 1)]] A_m(1; \delta) + \\ &\quad \frac{1}{2} [Ei[-\delta(\lambda_0 + 1)] - Ei(-2\delta)] A_m(-1; \delta) - \\ &\quad Q_0(\lambda_0) A_m(\lambda_0; \delta) + \frac{1}{2} G_m \end{aligned} \quad (\text{A8})$$

where  $\gamma$  is Euler's constant,  $Ei(x)$  is the exponential integral, and

$$G_m = (m!/\delta^{m+1}) \sum_{\nu=0}^m \delta^\nu \sum_{s=1}^{\nu} [s(\nu-s)! \delta^s]^{-1} \left[ \sum_{k=0}^{s-1} K_{\nu sk}(\delta) - e^{-\delta} \right] \quad (\text{A9})$$

$$K_{\nu sk}(\delta) =$$

$$(\delta^k/k!) \{ 2^k e^{-\delta} (-1)^{\nu-s} + e^{-\delta\lambda_0} [(\lambda_0 - 1)^k - (-1)^{\nu-s} (\lambda_0 + 1)^k] \} \quad (\text{A10})$$

Only the  $Z^p$  integrals with  $p = 0$  and  $p = -1$  are required since all others can be generated from those by a recursion relation.<sup>14</sup> Since the integrals depend only on the exponent  $\delta$  and the box parameter  $\lambda_0$ , the calculation can be most efficiently organized by tabulating the  $Z^p$  integrals for each specified pair of  $\delta, \lambda_0$  values.

## Appendix B

For the variational wave function used here, the average kinetic energy  $\bar{T}$  has the form

$$\bar{T} = f(\alpha, \lambda_0) / R^2 \quad (\text{B1})$$

with  $f(\alpha, \lambda_0)$  independent of  $R$ . For two noninteracting electrons in a spheroidal box, where the total energy is just the kinetic energy, the variational minimum occurs at the same  $\alpha$  and  $\{\lambda_k\}$  for all box sizes with the same  $\lambda_0$  (note that  $1/\lambda_0$  is the eccentricity), and

$$\bar{T}_e = F/R^2 = E_e \quad (\text{B2})$$

where  $F$  is a constant dependent on  $\lambda_0$ . The pressure  $P = -\partial E/\partial V$  is given by

$$P = (4/\pi)(R\lambda_0)^{-3} T \quad (\text{B3})$$

The kinetic energy can thus be rewritten as

$$\bar{T}_e = (\pi/4)^{2/5} (\lambda_0^2 F)^{3/5} P^{2/5} \quad (\text{B4})$$

and for a given  $\lambda_0$  the constant factor  $\lambda_0^2 F$  can be determined from a calculation for two noninteracting electrons in any size box.

The kinetic energy for two interacting electrons ( $H = T + 1/r_{12}$ ) was evaluated for several box sizes (in the range  $R\lambda_0 = 2-12$ ) and found to have essentially the same pressure dependence as that for two noninteracting electrons.